Article

J. Biol. Regul. Homeost. Agents. 2024; 38(6): 4639–4651
https://doi.org/10.23812/j.biol.regul.homeost.agents.20243806.369

Investigating the Prognostic Potential of ABTB1 Identified as a Hub Gene in B-Cell Acute Leukemia through Bioinformatics Analysis

Yan Luo[1,2,3], Cui Liu[2,3], Pei Huang[2,3], Jing Wang[2,3], Xin Xie[2], Yan Chen[2,*], Zhixu He[1,2,3,4,*]

[1]Suzhou Medical College of Soochow University, 215325 Suzhou, Jiangsu, China
[2]Department of Pediatrics, Affiliated Hospital of Zunyi Medical University, 563000 Zunyi, Guizhou, China
[3]Department of Pediatrics, Guizhou Children's Hospital, 563000 Zunyi, Guizhou, China
[4]Collaborative Innovation Center, Tissue Damage Repair and Regeneration Medicine, Zunyi Medical University, 563003 Zunyi, Guizhou, China
*Correspondence: cyz600@163.com (Yan Chen); hzx@gmc.edu.cn (Zhixu He)
Submitted: 9 January 2024 Revised: 29 February 2024 Accepted: 5 March 2024 Published: 1 June 2024

Background: Although some studies have highlighted the potential tumor-suppressive role of Ankyrin repeat and BTB/POZ domain-containing protein 1 (ABTB1) in various malignancies, its significance in B-cell acute lymphoblastic leukemia (B-ALL) remains unclear. This study aimed to explore the potential of ABTB1 as a prognostic marker for B-ALL.

Methods: Firstly, we identified differentially expressed genes (DEGs) in a patient with recurrent B-ALL, encompassing recurrence and complete remission, using bioinformatics methods. A protein-protein interaction (PPI) network for the identified DEGs was constructed using the Search Tool for Recurring Instances of Neighbouring Genes (STRING) database and visualized using Cytoscape software. Hub gene analysis was conducted utilizing three distinct algorithms (Degree, Maximal Clique Centrality (MCC), and Density of Maximum Neighborhood Component (DMNC)) via the cytoHubba plugin. The top 15 genes identified by each algorithm were designated as hub genes. Subsequently, transcriptome and clinical data from the TARGET database were then retrieved. mRNA expression profiles from 199 B-ALL cases were subjected to univariate Cox analysis to identify prognostic gene markers. Hub genes ($p < 0.05$) were then isolated from this gene pool. Kaplan-Meier analysis was conducted to examine the association between the extracted hub genes and overall survival (OS). Further screening of OS-related hub genes, considering hazard ratios from univariate Cox analysis and the regulatory patterns of DEGs, identified potential prognostic biomarkers. Finally, the expressions of the screened hub genes were validated, and their clinical significance was assessed in paediatric B-ALL patients.

Results: A total of 2666 DEGs were identified, comprising 930 upregulated and 1736 downregulated genes. Three candidate hub genes, namely *ABTB1* (Hazard Ratio (HR) = 0.683, $p < 0.05$), a disintegrin and a metalloproteinase domain-8 (ADAM8) (HR = 0.729, $p < 0.05$), and G protein-coupled 84 (*GPR84*) (HR = 0.868, $p < 0.05$), were markedly downregulated and associated with poor prognosis in B-ALL. Subsequent validation revealed that only *ABTB1* was differentially expressed between newly diagnosed B-ALL patients and those with complete remission. Furthermore, *ABTB1* exhibited significant associations with white blood cell count and risk stratification. Additionally, the protein expression of *ABTB1* was reduced in newly diagnosed B-ALL patients.

Conclusions: *ABTB1* emerges as a promising novel prognostic biomarker in B-ALL, shedding light on its potential role in disease progression and prognosis.

Keywords: ABTB1; acute lymphoblastic leukemia; B-cell acute lymphoblastic leukemia; prognostic biomarker

Introduction

Acute lymphoblastic leukemia (ALL) represents the most prevalent malignant hematological tumor among pediatric leukemia cases [1]. Originating from the abnormal proliferation of immature lymphoid cells, ALL leads to their accumulation within the bone marrow and extramedullary regions and their infiltration into various tissues and organs, suppressing normal hematopoietic function [1–3]. ALL is classified into B-cell ALL (B-ALL) and T-cell ALL (T-ALL) based on distinct cell origins, with B-ALL comprising approximately 85% of cases [1,4]. Remarkable advancements in treatment strategies, risk stratification, central nervous system prophylaxis, and minimal residual disease (MRD) monitoring have culminated in a 5-year survival rate of 90% in pediatric B-ALL patients [5–9]. Notably, St. Jude Hospital has achieved an exceptional 94.3% survival rate [10]. However, a significant proportion of B-ALL patients still face suboptimal treatment outcomes and relapses [6–8]. Furthermore, while chemotherapy remains the primary treatment approach, patient tolerance has nearly reached its threshold [10]. High-risk B-ALL patients undergoing intensive chemotherapy often endure reduced

Journal of
BIOLOGICAL REGULATORS
and Homeostatic Agents

quality of life due to a spectrum of complications [10]. Consequently, there exists an imperative to explore innovative treatment approaches that can enhance efficacy while mitigating adverse reactions.

Contemporary research underscores the potential benefits of integrating chemotherapy with targeted therapies, offering improved disease-free survival and overall survival (OR) rates while significantly reducing toxicity and enhancing MRD clearance, presenting a promising avenue for B-ALL patients [11]. Noteworthy among these targeted therapies is the application of tyrosine kinase inhibitors in Philadelphia chromosome-positive (Ph+) ALL, characterized by the BCR-ABL fusion gene, which has raised the 5-year event-free survival (EFS) from the initial 30% to the current 80% [12–14]. Additionally, BCL-2 inhibitors, alone or in combination with other agents, have emerged as a novel targeted therapy for ALL, effectively attenuating leukemia progression despite the notable side effect of thrombocytopenia [15,16]. Furthermore, research has demonstrated that combining another BCL-2 inhibitor, Venetoclax, with nelarabine enhances chemotherapy sensitivity, improves drug responsiveness, and diminishes chemotherapy-related side effects dependent on dosage [17]. Thus, delving deeper into the molecular mechanisms of B-ALL and exploring novel therapeutic targets associated with prognosis may represent a potent strategy for enhancing the quality of life and survival rates among B-ALL patients.

High-throughput sequencing technology and bioinformatics analysis are pivotal tools for identifying tumor-specific genes and prognostic biomarkers, advancing cancer treatment [18]. This approach is widely applied in exploring disease pathogenesis, molecular diagnosis, treatment targets, and prognosis prediction [18]. The molecular mechanisms underlying acute leukemia are closely related to gene mutations, deletions, and expression imbalances [8,19]. Scholars have identified prognostic biomarkers from leukemia samples using bioinformatics and high-throughput sequencing, improving risk stratification, and enhancing cure rates for pediatric patients [20–25]. Hence, employing high-throughput sequencing and bioinformatics to identify molecular participants is indispensable for gaining deeper insights into B-ALL pathogenesis and developing personalized treatment strategies.

In this study, we collected specimens from a recurrent B-ALL patient with unidentified pathogenic genes. By comparing RNA expression profiles between recurrent and remission stages using transcriptome data from the patient and integrating transcriptome data and clinical information from 199 B-ALL patients in the TARGET database, we identified three candidate hub genes, namely Ankyrin repeat and BTB/POZ domain-containing protein 1 (ABTB1), a disintegrin and a metalloproteinase domain-8 (ADAM8), G protein-coupled 84 (GPR84) as novel B-ALL biomarkers through bioinformatics analysis. Subsequently, we observed only ABTB1 was differentially expressed between newly diagnosed B-ALL patients and those with complete remission in the verification experiment. Additionally, we observed a significant downregulation of ABTB1 mRNA and protein levels in bone marrow specimens from B-ALL patients. Low ABTB1 expression was closely associated with poor prognosis in the TARGET database. In summary, these findings suggest that ABTB1 holds promise as a potential target for treating B-ALL.

Materials and Methods

RNA Sequencing and DEG Identification

In compliance with the guidelines of the Declaration of Helsinki, informed consent was obtained from all participants. Additionally, approval was obtained from the Ethics Committee of the Affiliated Hospital of Zunyi Medical University (Approval No. KLL-2021-353) for all laboratory experiments involving primary samples and data. For this study, a recurrent B-ALL patient lacking a known pathogenic gene was enrolled. Total RNA was extracted from bone marrow mononuclear cells (BM-MNC) during the relapse and remission stages using Trizol (15596-018, Invitrogen, Carlsbad, CA, USA), following the manufacturer's instructions. Subsequently, RNA sequencing was performed using the Illumina sequencing platform. The RNA library was prepared according to the protocol provided by the Next® Ultra™-RNA-Library-Prep-Kit-for-Illumina® (NEB, Ipswih, MA, USA). The library was then subjected to high-throughput sequencing using the Illumina NovaSeq 6000 platform. To ensure high-quality data (Clean Data), offline quality control was conducted on the original sequencing data, involving the removal of low-quality bases, splices, and shear ends. Subsequently, the Clean Data was aligned to the specified reference genome (https://ftp.ensembl.org/pub/release-103/fasta/homo_sapiens/dna/Homo_sapiens.GRCh38.dna.toplevel.fa.gz) using HiSat2, resulting in mapped data (Reads) for subsequent transcript assembly and expression calculations.

Differential expression analysis was performed using the "EBSeq.2" package in R 4.0.3 software (https://www.r-project.org/) with criteria set at p-adjust < 0.01 and $|\log2 FC| > 2$ to identify differentially expressed genes (DEGs). The entire RNA sequencing workflow, encompassing total RNA extraction, quality assessment, RNA library preparation, sequencing, and DEG screening, was conducted by Beijing Qingke Biotechnology Limited Company.

Establishing the Protein-Protein Interaction (PPI) Network and Identifying Hub Genes

This study constructed a PPI network for DEGs using the Search Tool for Recurring Instances of Neighbouring Genes (STRING) database (https://string-db.org/). Subsequently, the stringApp in Cytoscape software (v3.8.2, https://www.cytoscape.org/) was employed to generate the

PPI network for DEGs with default settings. The PPI network was visualized based on the Degree value of each gene [26,27]. Three algorithms were employed to identify potential prognostic biomarkers for B-ALL: Degree, Maximal Clique Centrality (MCC), and Density of Maximum Neighborhood Component (DMNC), in the cytoHubba plugin provided by Cytoscape software for hub genes screening [28].

Screening of OS-Related Genes via Univariate Cox Analysis in the TARGET Database and Identification of Hub Genes

A total of 312 transcriptome datasets of ALL were retrieved from the TARGET database as of October 7, 2022 (https://ocg.cancer.gov/programs/target). It is noteworthy that the TARGET database predominantly focuses on pediatric tumors. Associated clinical parameters were also obtained from the same source, encompassing parameters such as overall survival time, survival status, and immune subtypes of ALL. Any datasets with ambiguous clinical staging or unknown prognostic information were excluded from the analysis. Additionally, clinical parameters of 199 B-ALL cases were extracted from the ALL clinical data. Notably, ethics committee approval was not required for this research, as all utilized data were publicly available.

The following steps were undertaken to identify the genes associated with overall survival (OS) in B-ALL transcriptome datasets from the TARGET database: Firstly, the Perl programming language (https://www.perl.org/) was used to retrieve the initial transcript data for ALL transcriptome samples. Subsequently, the expression profiles were annotated based on the "GRCH38.95.chr.gtf.GZ" file obtained from the Ensembl database (https://asia.ensembl.org/index.html). Duplicate genes were removed, and the mRNA expression profile matrix was derived from the transcriptome data using a Perl script. Next, the survival status and period obtained from the clinical data of B-ALL patients were integrated with the mRNA expression profile matrix of ALL. Univariate Cox analysis was conducted to identify genes significant for establishing reliable prognostic markers using the "survival" package in R 4.1.2 software (https://www.r-project.org/). Finally, hub genes were extracted from the selected pool of genes associated with OS, considering a p-value less than 0.05, and designated as the "A" group.

Screening of OS-Related Genes through Kaplan-Meier Analysis Using the TARGET Database

We conducted an extensive analysis in the TARGET database to further refine our search for potential prognostic markers associated with OS in B-ALL. Kaplan-Meier survival analysis was performed on genes within the "A" group, subsequently identifying hub genes with a significance level of $p < 0.05$. These hub genes were designated as the "B" group.

Screening for Potential Prognostic Biomarkers in the "B" Group Based on HR Values Obtained in Univariate Cox Analysis and Regulatory Patterns of DEGs

The Hazard Ratio (HR) derived from univariate Cox analysis indicates the impact of exposure relative to the control group concerning the occurrence of positive events. When HR exceeds 1, it indicates that the exposure factors promote the occurrence of positive events. Conversely, HR values below 1 indicate that exposure factors suppress the occurrence of positive events. If the HR equals 1, it suggests that exposure factors do not influence positive event occurrence. Notably, in our study, HR values exceeding 1 in univariate Cox analysis indicate that higher gene expression levels correspond to an increased risk of B-ALL occurrence. Conversely, HR values below 1 suggest that lower gene expression levels are associated with an increased probability of B-ALL occurrence. To implement this concept, we utilized the R package "Venn Diagram" (R version 4.1.2) to identify the overlap of genes meeting two criteria in the "B" group: those exhibiting HR values exceeding 1 (indicating increased B-ALL probability) and those classified as upregulated genes, which may facilitate tumorigenesis among DEGs. Additionally, we employed the same package to identify the intersection of genes meeting two other criteria in the "B" group: those with HR values below 1 (indicating increased B-ALL probability) and those classified as downregulated genes, and the down-regulation of these cross genes may potentially promote tumorigenesis.

Collection of Bone Marrow Samples and Clinical Data from B-ALL Patients for Verification of Identified Hub Genes

To verify the expression levels of the identified hub genes, the bone marrow specimens were collected from B-ALL patients who were newly diagnosed or experiencing relapse at the Pediatric Department of Zunyi Medical University Affiliated Hospital between January 2018 and August 2022. Additionally, bone marrow samples were collected from B-ALL patients who had achieved complete remission during this period, and from healthy donors. The samples included 36 newly diagnosed patients, 5 relapse cases, 29 patients in complete remission, and 8 healthy donors. Bone marrow mononuclear cells were isolated using a human lymphocyte isolation solution and transferred into RNA-free Eppendorf (EP) tubes. Subsequently, 1 mL of Trizol was added and thoroughly mixed, and the specimens were stored in a –80 °C refrigerator for future analyses. The inclusion criteria were: (1) Newly diagnosed B-ALL patients were classified according to MICM standards, including bone marrow cytology, immune classification, cytogenetics, and molecular abnormalities [29]; (2) Patients who had experienced relapse; (3) Patients aged under 18 years. For relapse criteria, the reappearance of the disease at any location after a phase of complete remission,

Journal of
BIOLOGICAL REGULATORS
and Homeostatic Agents

occurring during or after initial therapy, was considered [30]. The exclusion criteria were: (1) Cases where bone marrow samples were not obtainable due to aspiration challenges; (2) Patients who had undergone chemotherapy; (3) Samples with mRNA quality that did not meet the required standards; (4) Patients concurrently diagnosed with other tumors.

Additionally, to explore the association between the hub genes and clinical parameters of B-ALL patients, we collected essential clinical data, including gender, age, survival status, survival time, risk stratification, white blood cell counts (WBC), bone marrow leukemic blast count, and chromosome karyotype (Table 1). Notably, all laboratory experiments involving primary specimens received approval from the Medical Ethics Committee of the Affiliated Hospital of Zunyi Medical University (Approval No. KLL-2021-353).

Table 1. Clinical features of B-ALL patients.

Characteristic	Number of cases (%)
Age (years)	
>10	2 (5)
≤10	38 (95)
Gender	
Male	21(52.5)
Female	19 (47.5)
WBC ($\times10^9$/L)	
≤30	26 (65)
>30	14 (35)
Anemia	
Yes	39 (97.5)
No	1 (2.5)
PLT ($\times10^9$/L)	
<100	28 (70)
≥100	12 (30)
Blast in Bone Marrow (%)	
≤50	3 (7.5)
50–100	37 (92.5)
Risk Classification of B-ALL	
High Risk	13 (32.5)
Middle Risk	17 (42.5)
Low Risk	10 (25)
Gene Mutation	
Abnormal	12 (42.9)
Normal	16 (57.1)
Fusion Gene	
Abnormal	12 (32.4)
Normal	25 (67.6)
Karyotype	
Abnormal	12 (46.2)
Normal	14 (53.8)

WBC, white blood cell counts; PLT, platelet; B-ALL, B-cell acute lymphoblastic leukemia.

Cell Culture

Acute leukemia cell lines, namely, Nalm6 (iCell-h149), BALL-1 (iCell-h283), and Reh (iCell-h181), were provided by iCell Bioscience Inc (Shanghai, China). CEM-C1 and CEM-C7 were generously provided by Professor Zhigui Ma (West China Second University Hospital). Subsequently, STR and mycoplasma identification were conducted for all the cell lines, confirming their genetic profiles and ruling out any Mycoplasma contamination. The cells were cultured in a complete 1640 solution supplemented with 10% fetal bovine serum (FBSAD-01011, OriCell®, Guangzhou, China), 0.1 mg/mL streptomycin (P1400, Solarbio, Beijing, China), and 100 U/mL penicillin (P1400, Solarbio, Beijing, China), and cultured under a 5% CO_2 atmosphere and 37 °C.

Quantitative Reverse Transcription PCR (RT-qPCR)

Total RNA was isolated using RNAiso plus (9109, Takara, Dalian, China), and subsequent reverse transcription was performed using the PrimeScript™ RT reagent Kit with gDNA Eraser (RR047A, Takara, Dalian, China). RT-qPCR was conducted on LightCycler® 480 System using the TB Green Premix Ex Taq (2×) (RR820, Takara, Dalian, China) with specific primers as outlined in Table 2. Beta-actin (*ACTB*) served as an internal control, with each sample undergoing amplification in a 10 µL reaction volume according to the manufacturer's instructions. Relative expression levels of target genes were analyzed using the $2^{-\Delta\Delta Ct}$ method.

Table 2. RT-qPCR primers.

Primer Name	Sequence (5′-3′)
ABTB1 (homo)-F	GACGTCTTCACTCACGTGCTCT
ABTB1 (homo)-R	CAGTGTCCTCGTCTAGCATCTGA
ADAM8 (homo)-F	GGTGAATCACGTGGACAAGCTA
ADAM8 (homo)-R	CAGGTCAGGAGGTTCTCCAGTG
GPR84 (homo)-F	AACGAGCAGCACAGGCACT
GPR84 (homo)-R	CAGCACTGACTGGCTCAGA
ACTB (homo)-F	TTCCTTCCTGGGCATGGAGT
ACTB (homo)-R	GACAGCACTGTGTTGGCGTA

RT-qPCR, Quantitative Reverse Transcription PCR; *ABTB1*, Ankyrin repeat and BTB/POZ domain-containing protein 1; *ACTB*, Beta-actin; *ADAM8*, a disintegrin and a metalloproteinase domain-8; *GPR84*, G protein-coupled 84.

Western Blotting

150 µL of Radio Immunoprecipitation Assay (RIPA) buffer (Cat: R0010, Solarbio, Beijing, China) was added to the harvested cells (cell count was 1×10^7), followed by lysis on ice for 30 minutes. Subsequently, the lysate was centrifuged at 12,000 g for 30 minutes at 4 °C, and the resulting supernatant was collected. The protein concentration of the

supernatant was determined using the BCA method (Cat: GK5012, GENEray™, Shanghai, China). After quantifying the proteins, 5× loading buffer was added to the total protein, and place the mixture in boiling water at 100 °C for 5–8 minutes. The protein samples were then separated using 10% SDS-polyacrylamide gels and transferred onto a polyvinylidene fluoride (PVDF, IPVH00010, Millipore, Shanghai, China) membrane. After blocking with 5% skim milk for 2 hours, the membrane was incubated at 4 °C with the appropriate primary antibodies for 15–17 hours. Subsequently, the blots were rinsed, and the membrane was incubated with the HRP conjugated goat anti-Rabbit IgG secondary antibody (1:10,000, HA1001, HuaAn, Hangzhou, China) for 1 hour. Finally, the image was obtained using the ChemiDoc™ imaging system (BIO-RAD, Berkeley, CA, USA). The primary antibodies included ABTB1 Antibody (1:1000, bs-12881R, Abbkine, Beijing, China) and Glyceraldehyde-3-phosphate dehydrogenase (GAPDH) Antibody (1:10,000, ET1601-4, HuaAn, Hangzhou, China). GAPDH was served as the loading control.

Statistical Methods

Statistical analysis was conducted using Perl software (v5.34.1) (https://www.perl.org), R v4.1.2 (https://www.r-project.org/), SPSS software (v22.0, IBM, Armork, NY, USA), and GraphPad Prism Software (v8.0.2, La Jolla, CA, USA). Various packages, including "survival", "limma", "ggplot", and "pheatmap", were employed for data analysis and visualization. Differences between two groups were analyzed using the unpaired Student *t*-test with normally distributed data and the data was presented as mean ± standard error (SEM). If the data was non-normal distributed, the Mann-Whitney U test was used for cases between two groups, and the data was presented as median with interquartile range. For multiple groups, one-way ANOVA was applied, followed by LSD test with normally distributed data; and kruskal-wallis test was used for data with non-normal distributed. Pearson's chi-square test or Fisher's exact test were utilized for comparing categorical variables. Bivariate correlations between study variables were calculated using Spearman's rank correlation test. A significance threshold of $p < 0.05$ was adopted to determine statistical significance.

Results

Identification of DEGs

Using the "EBseq2" software package, we identified 2666 DEGs from the transcriptome data of BM-MNC obtained from a relapsed B-ALL patient at the remission and recurrence stages. The DEGs comprised 930 upregulated and 1736 downregulated genes. Further evaluation and visualization of the DEGs were performed using a Minus-versus-Add (MA) plot and a heatmap (Fig. 1A,B). The MA plot illustrates the distribution of DEGs after normalization (Fig. 1A), while the heatmap demonstrates the expression levels of DEGs (Fig. 1B).

Protein-Protein Interaction (PPI) Network and Hub Gene Analysis of DEGs

A PPI network for DEGs was constructed using the STRING database and the stringApp in Cytoscape 3.8.2 software with default settings. The PPI network was visualized based on the node degree of each gene (Fig. 2A). The PPI network comprised 928 nodes and 4435 edges. Additionally, cytoHubba, a plugin in Cytoscape software, offers topological analysis methods to identify crucial genes within the network, designating them as hub genes [28]. Thus, we identified hub genes using three different algorithms, namely, Degree, MCC, and DMNC, through the cytoHubba plugin. The top 15 core genes of each algorithm are presented in Table 3 and visualized in Fig. 2B–D.

Survival Analysis: Validation of Hub Genes by Univariate Cox Analysis and Kaplan-Meier Analysis in the TARGET Database

We conducted a comprehensive analysis of genes retrieved from the TARGET database. Univariate Cox analysis was employed to identify 7444 genes significantly correlated with OS in B-ALL patients ($p < 0.05$). To identify OS-related genes among the hub genes presented in Table 3, we extracted those ($p < 0.05$) from 7444 genes associated with the OS in B-ALL in the TARGET database. Our screening revealed 17 hub genes potentially relevant to B-ALL prognosis. The identified genes include *ABTB1*, *DCAF12*, *BRI3*, *NFAM1*, *ABCA13*, *EGF*, *FPR2*, *C3AR1*, *PPBP*, *ELANE*, *CKAP4*, *LYZ*, *RETN*, *STOM*, *ADAM8*, *GPR84*, and *SLC2A3* (Table 4). Among the genes, *ABTB1*, *ABCA13*, *EGF*, *ADAM8*, *GPR84*, and *SLC2A3* exhibited Hazard Ratio (HR) values less than 1, suggesting that lower expression levels of these genes may be associated with a higher risk of B-ALL development (Table 4). Conversely, *DCAF12*, *BRI3*, *NFAM1*, *FPR2*, *C3AR1*, *PPBP*, *ELANE*, *CKAP4*, *LYZ*, *RETN*, and *STOM* had HR values greater than 1, indicating that higher expression levels of these genes may contribute to the onset of B-ALL (Table 4).

To further investigate the association between the 17 hub genes and OS, we classified them into low- and high-expression groups based on the median value. Utilizing the "survival" package, we conducted Kaplan-Meier analysis to draw survival curves using data from the TARGET database (the clinical parameters of the B-ALL patients and expression levels of the genes are presented in the **Supplementary Material**). The results revealed that 14 genes, namely *ABTB1*, *ABCA13*, *NFAM1*, *BRI3*, *ADAM8*, *CKAP4*, *EGF*, *ELANE*, *FPR2*, *GPR84*, *LYZ*, *PPBP*, *RETN*, and *STOM*, were significantly related to OS ($p < 0.05$) (Fig. 3), and were designated as the "C" group. Our findings suggest that elevated expression levels of *NFAM1*, *BRI3*,

Journal of
BIOLOGICAL REGULATORS
and Homeostatic Agents

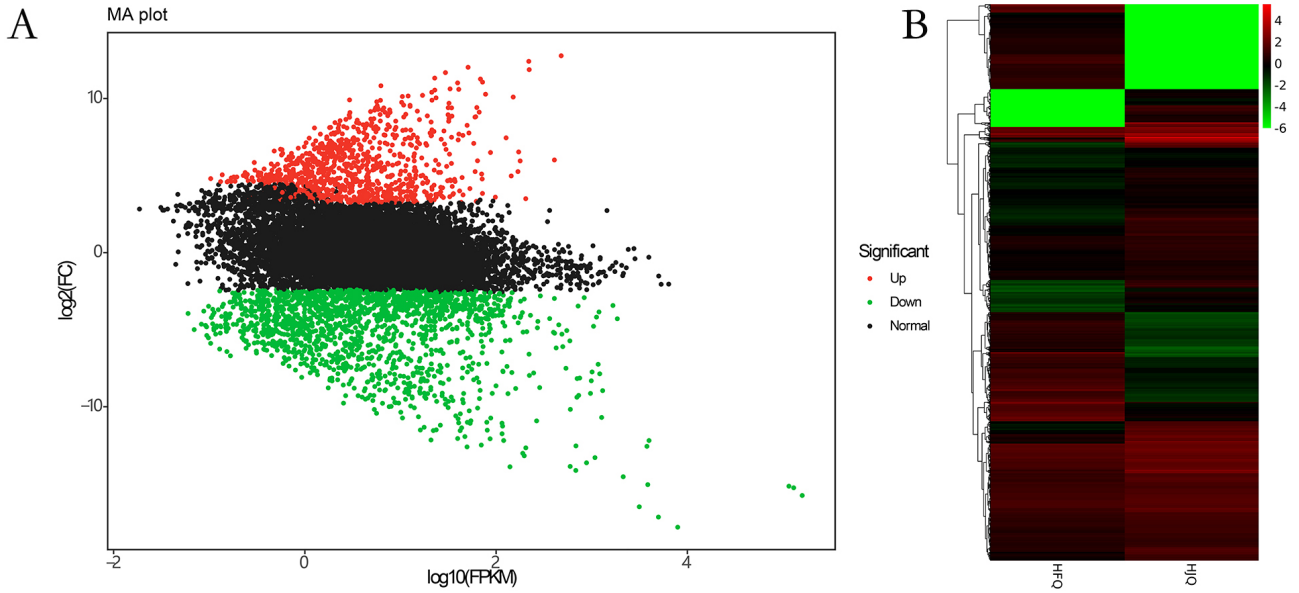

Fig. 1. Identification of differentially expressed genes (DEGs) in relapsed B-cell acute lymphoblastic leukemia (B-ALL) patient between the recurrent stage and remission. (A) Minus-versus-Add (MA) plot of the DEGs. Red and green dots indicate upregulated and downregulated genes, respectively. (B) Heatmap of the DEGs. HFQ represents the sample from the recurrent stage, while HJQ represents the sample obtained from the complete remission stage. The color band indicates the expression level of genes, where red and green represent high and low expression, respectively.

Table 3. Hub genes in the DEGs identified using the Degree, DMNC, and MCC algorithms in the cytoHubba plugin of Cytoscape software.

Parameters	Gene names
Degree	*EGF*, *MMP9*, *FPR2*, *LRRK2*, *CXCL1*, *ITGB2*, *C3AR1*, *QSOX1*, *PPBP*, *CDH1*, *ORM2*, *ELANE*, *CKAP4*, *LYZ*, *RENT*
MCC	*FPR2*, *C3AR1*, *STOM*, *ITGB2*, *ADAM8*, *CD177*, *CLEC4D*, *CLEC5A*, *FCAR*, *GPR84*, *MCEMP1*, *PTPRB*, *SLC2A3*, *CLEC12A*, *ATP8B4*
DMNC	*IL1R2*, *DCAF12*, *F13A1*, *NFAM1*, *ADGRA3*, *LTBR*, *TNFSF14*, *BRI3*, *ABTB1*, *ACP3*, *DCAF11*, *CELSR2*, *ABCA13*, *LAMB4*, *MMRN1*

CKAP4, *ELANE*, *FPR2*, *LYZ*, *RETN*, *PPBP*, and *STOM* are associated with poor prognosis, while the decreased expression levels of *ABTB1*, *ABCA13*, *ADAM8*, *EGF*, *GPR84*, and *SLC2A3* are associated with poor prognosis (Fig. 3).

We performed an intersection to identify the most promising hub genes related to OS. We selected genes in the "C" group with HR values greater than 1 from Table 4 and intersected them with upregulated genes among the DEGs, likely to promote tumorigenesis. Similarly, we identified genes in the "C" group with HR values less than 1 from Table 4 and intersected them with downregulated DEGs. Ultimately, we identified three hub genes among the downregulated DEGs as potential prognostic biomarkers, namely, *ABTB1*, *ADAM8*, and *GPR84* (Fig. 4A,B). These genes may serve to suppress tumorigenesis.

Verification of mRNA Expression of Screened Hub Genes in B-ALL Patients

A comprehensive analysis was conducted to assess the mRNA expression of the identified hub genes in B-ALL patients. Our study examined mRNA levels in bone marrow samples from newly diagnosed B-ALL patients, those in complete remission, and healthy donors (the control group). Our findings revealed a significant downregulation in the expression of *ABTB1* in newly diagnosed B-ALL patients compared to healthy donor and complete remission groups ($p < 0.05$, Fig. 5A). However, no apparent difference was observed in the mRNA levels of *ADAM8* and *GPR84* when comparing newly diagnosed B-ALL patients to the complete remission group ($p > 0.05$, Fig. 5B,C).

Furthermore, our investigation extended to relapsed B-ALL patients. Compared to the control and complete remission groups, ABTB1 remained downregulated in relapsed B-ALL patients ($p < 0.05$, Fig. 5D), while no significant difference was observed between patients in complete remission and the control subjects ($p > 0.05$, Fig. 5D). Additionally, we evaluated ABTB1 protein expression, indicating a decrease in ABTB1 protein levels among newly diagnosed B-ALL patients (Fig. 5E). To gain further insight, we assessed ABTB1 expression in ALL cell lines. The

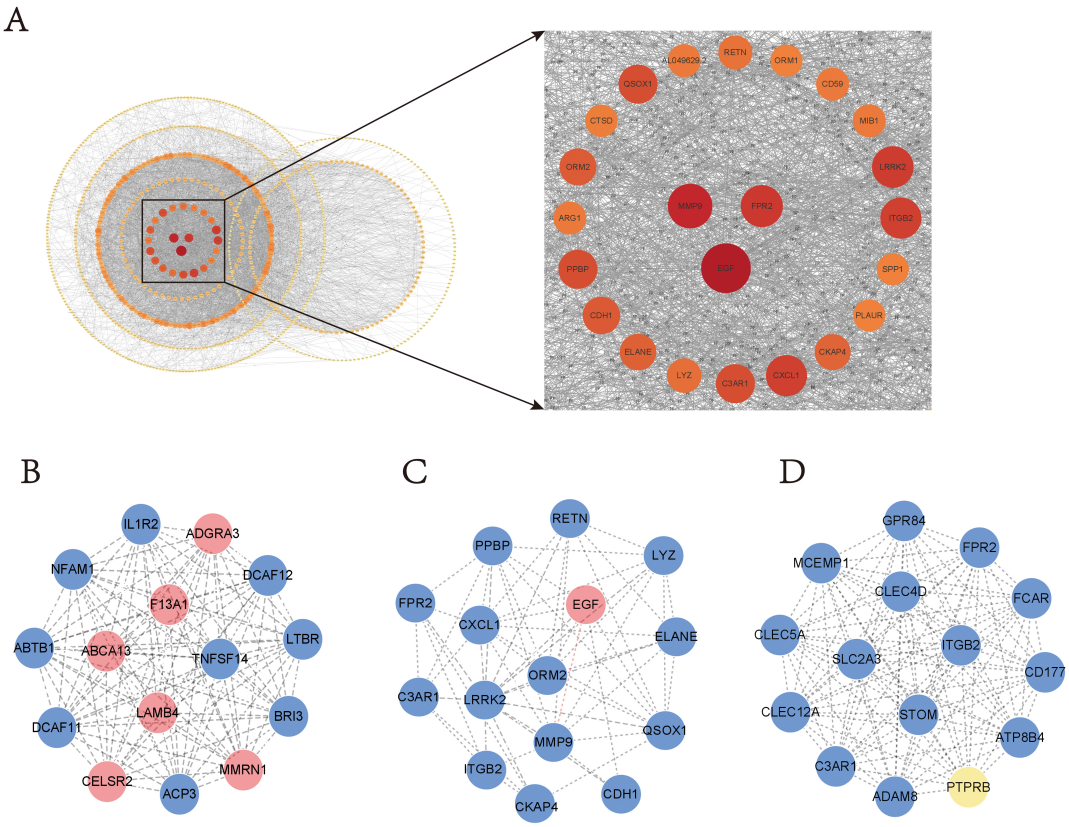

Fig. 2. Protein-protein interaction (PPI) network for the 2666 DEGs retrieved from the Search Tool for Recurring Instances of Neighbouring Genes (STRING) database, with key sub-networks and nodes identified from the cytoHubba plugin based on three topological algorithms. The top 15 hub genes were screened from the key sub-networks of the PPI network using each of the three topological algorithms, namely Density of Maximum Neighborhood Component (DMNC), Degree, Maximal Clique Centrality (MCC). (A) PPI network obtained from the STRING database. The intensity of color in the network indicates its significance based on the algorithm used. Sub-networks and hub genes were obtained from the DMNC (B), Degree (C), and MCC (D) topological algorithms. Additionally, if genes in the sub-networks are downregulated among DEGs, they are shown in blue, while genes displayed in other colors are upregulated.

mRNA levels of *ABTB1* were consistently lower in ALL cell lines, including Nalm6, Ball-1, Reh, C1, and C7, compared to mononuclear cells from healthy individuals ($p < 0.05$, Fig. 5F). These findings suggest that *ABTB1* is downregulated in B-ALL. Its impact extends beyond the mRNA level to the protein level, and the diminished expression plays a pivotal role in the development of B-ALL.

Association between Downregulated ABTB1 and Advanced Clinicopathological Features of B-ALL

In the clinical landscape of leukemia, gender, age, white blood cell count, immune phenotype, risk stratification, chromosome, and genetic variations significantly influence the recurrence and mortality rates among pediatric leukemia patients [31]. Thus, we explored the potential association between ABTB1 expression and various clinicopathological features in B-ALL patients.

Table 5 shows significant correlations between ABTB1 expression and two specific factors: white blood cell count ($p = 0.047$) and risk stratification ($p = 0.018$). However, no significant associations were observed between ABTB1 expression and factors such as age ($p = 1.000$), gender ($p = 0.752$), platelet count ($p = 0.168$), BLAST count in bone marrow ($p = 0.548$), anemia ($p = 0.311$), gene mutations ($p = 0.702$), gene fusions ($p = 1$), or karyotype ($p = 0.453$).

Further Spearman correlation analysis was conducted to evaluate the relationship between ABTB1 expression and clinicopathological features. The findings confirmed that decreased ABTB1 expression was significantly correlated with elevated white blood cell count and higher risk stratification, underscoring the potential clinical relevance of ABTB1 in B-ALL (Table 6). These findings suggest a close association between ABTB1 expression and specific clinicopathological characteristics in B-ALL patients.

Journal of
BIOLOGICAL REGULATORS
and Homeostatic Agents

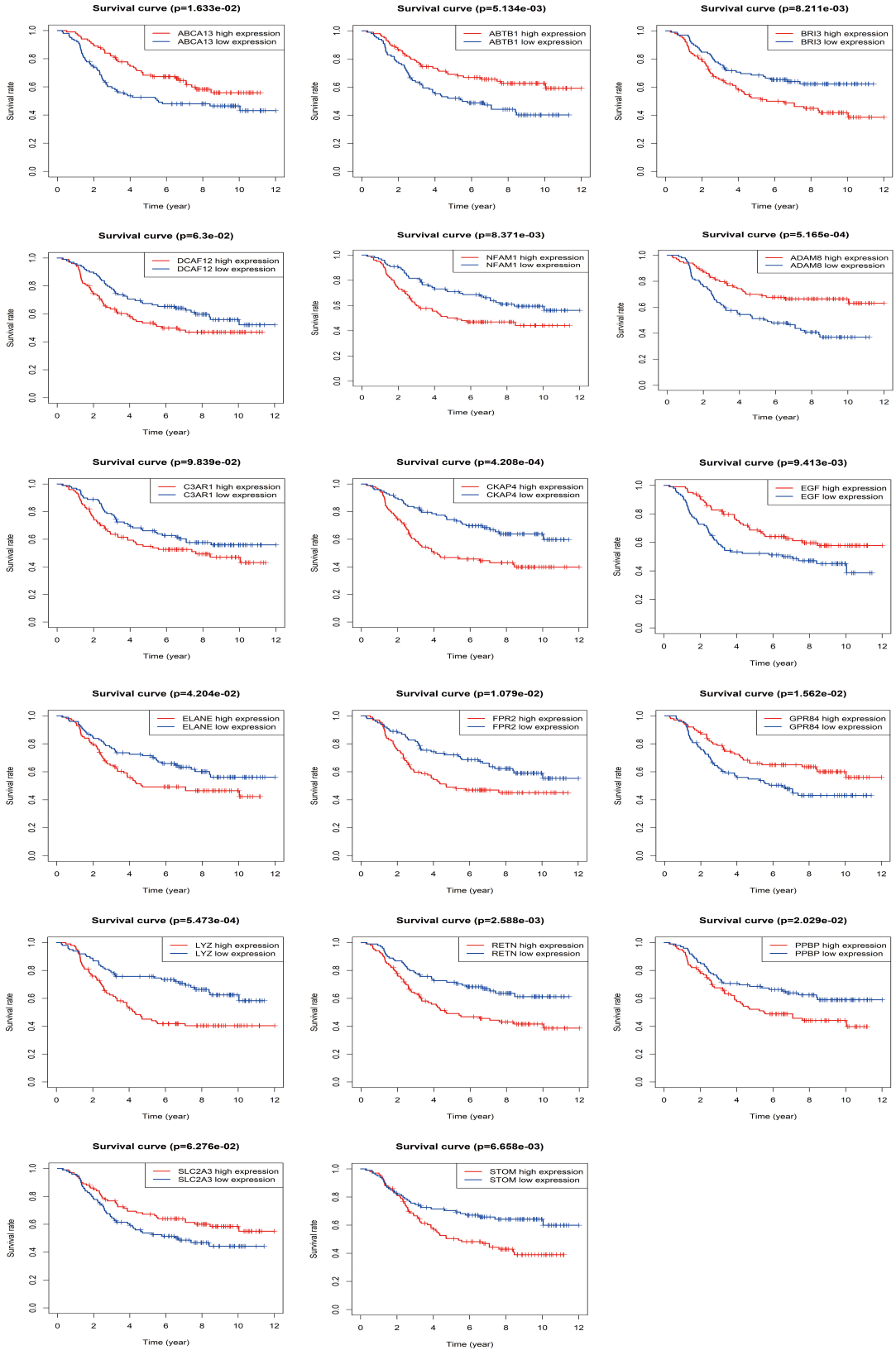

Fig. 3. Analysis of the relationship between hub genes including *ABTB1*, *DCAF12*, *BRI3*, *NFAM1*, *ABCA13*, *EGF*, *FPR2*, *C3AR1*, *PPBP*, *ELANE*, *CKAP4*, *LYZ*, *RETN*, *STOM*, *ADAM8*, *GPR84*, and *SLC2A3* and OS using Kaplan-Meier analysis in the TARGET database.

Table 4. Hub genes related to OS identified by univariate Cox analysis in the TARGET database.

Genes	HR (95% CI)	Z	*p*-value
ABTB1	0.683 (0.525, 0.890)	–2.821	0.005
DCAF12	1.252 (1.065, 1.471)	2.724	0.006
BRI3	1.338 (1.140, 1.571)	3.554	0.0004
NFAM1	1.119 (1.019, 1.228)	2.361	0.018
ABCA13	0.913 (0.852, 0.979)	–2.560	0.010
EGF	0.842 (0.766, 0.925)	–3.582	0.0003
FPR2	1.153 (1.060, 1.255)	3.304	0.001
C3AR1	1.193 (1.070, 1.330)	3.175	0.002
PPBP	1.091 (1.013, 1.174)	2.301	0.021
ELANE	1.102 (1.027, 1.183)	2.687	0.007
CKAP4	1.341 (1.171, 1.534)	4.258	2.06×10^{-5}
LYZ	1.167 (1.083, 1.256)	4.068	4.74×10^{-5}
RETN	1.097 (1.019, 1.182)	2.457	0.014
STOM	1.312 (1.090, 1.580)	2.869	0.004
ADAM8	0.729 (0.621, 0.855)	–3.876	0.0001
GPR84	0.868 (0.785, 0.956)	–2.782	0.005
SLC2A3	0.773 (0.655, 0.912)	–3.042	0.002

CI, confidence interval; OS, overall survival.

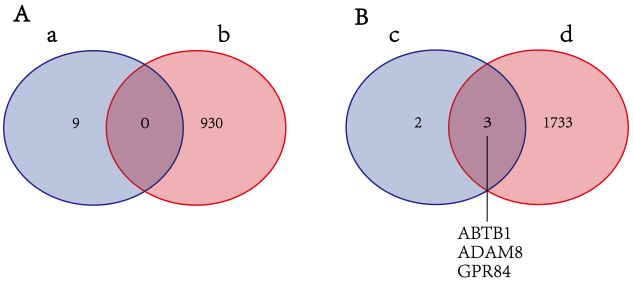

Fig. 4. Identification of hub genes related to OS. (A) The genes in the "C" group with HR >1 from Table 4 and intersected them with upregulated DEGs. The blue circle "a" indicates genes with HR >1, while the red circle "b" indicates upregulated DEGs. (B) The genes in the "C" group with HR <1 from Table 4 and intersected them with downregulated DEGs. The blue circle "c" represents genes with HR <1, while the red circle "d" indicates downregulated DEGs. HR, Hazard Ratio.

Discussion

B-cell acute lymphoblastic leukemia (B-ALL) stands as one of the most prevalent malignancies affecting children [11]. Despite significant advancements in current treatment modalities, including chemotherapy, which have notably improved remission and 5-year survival rates among pediatric B-ALL patients, this disease remains the leading cause of cancer-related mortality in children [32–35]. Jeha *et al.* [10] have highlighted that patients with B-ALL have reached the limits of tolerable chemotherapy intensity, necessitating exploration into novel treatment strategies. Increasingly, studies underscore the intricate molecular landscape of leukemia, characterized by gene deletions, amplifications, dysregulations, and epigenetic abnormalities, with growing evidence supporting the potential of molecularly targeted therapies [8,36,37]. Hence, the quest for new prognostic biomarkers from a molecular perspective enhances our understanding of B-ALL pathogenesis and holds promise for advancing personalized and precision therapies for pediatric B-ALL patients.

In this study, we employed bioinformatics methodologies to identify 2666 DEGs in patients with recurrent B-ALL during recurrence and complete remission phases. Subsequently, we constructed a PPI network for the DEGs using the STRING database. Through cytoHubba plugin within Cytoscape software, we identified the top 15 hub genes for each algorithm, including Degree, MCC, and DMNC algorithms. Subsequently, we conducted univariate Cox and Kaplan-Meier analyses to validate hub genes exhibiting significant associations with OS, identifying 14 hub genes ($p < 0.05$). Among these, 9 were upregulated in DEGs, while 5 were downregulated in DEGs. Based on HR values obtained in the univariate Cox analysis and the regulatory patterns of DEGs, we identified three promising candidate prognostic biomarkers.

Moreover, we observed a significant difference in the expression of these candidate hub genes between newly diagnosed B-ALL patients and the complete remission group, with only ABTB1 demonstrating statistical significance. Moreover, compared to the B-ALL remission group, we observed lower expression of ABTB1 in newly diagnosed and relapsed B-ALL patients, suggesting that the downregulation of ABTB1 in B-ALL may contribute to disease progression in pediatric B-ALL patients. Therefore, we propose that ABTB1 holds promise as a novel prognostic marker in B-ALL.

ABTB1, also known as BPOZ, is located on chromosome 3q21. Its cDNA sequence comprises an open reading frame of 1434 base pairs, encoding 478 amino acid residues [38]. Sequence pattern analysis reveals that ABTB1 consists of two BTB/POZ domains, a bipartite nuclear localization signal, and an N-terminal Ankyrin repeat [38]. Unoki *et al.* [39] have elucidated that ABTB1 consists of 12 exons, with exon 2 undergoing selective splicing to yield three transcripts: BPOZ-1/2/3. Among the splicing isomers derived from ABTB1, current research predominantly focuses on BPOZ-2. Previous research has demonstrated that overexpression of the BPOZ-2 splicing isomer in endometrial and ovarian cancer cell lines suppresses cell-cycle progression from G1 to S phase, significantly inhibiting the proliferation of these tumor cells [39]. Moreover, transfection of miR-439 into colorectal cancer cell lines SW480 and HCT116 suppresses cell proliferation, migration, and invasion while reducing ABTB1 levels, suggesting ABTB1 as a potential therapeutic target for colorectal cancer [40]. Additionally, Wan *et al.* [41] utilized the TCGA public database to construct a co-expression module via WGCNA and other

Journal of
BIOLOGICAL REGULATORS
and Homeostatic Agents

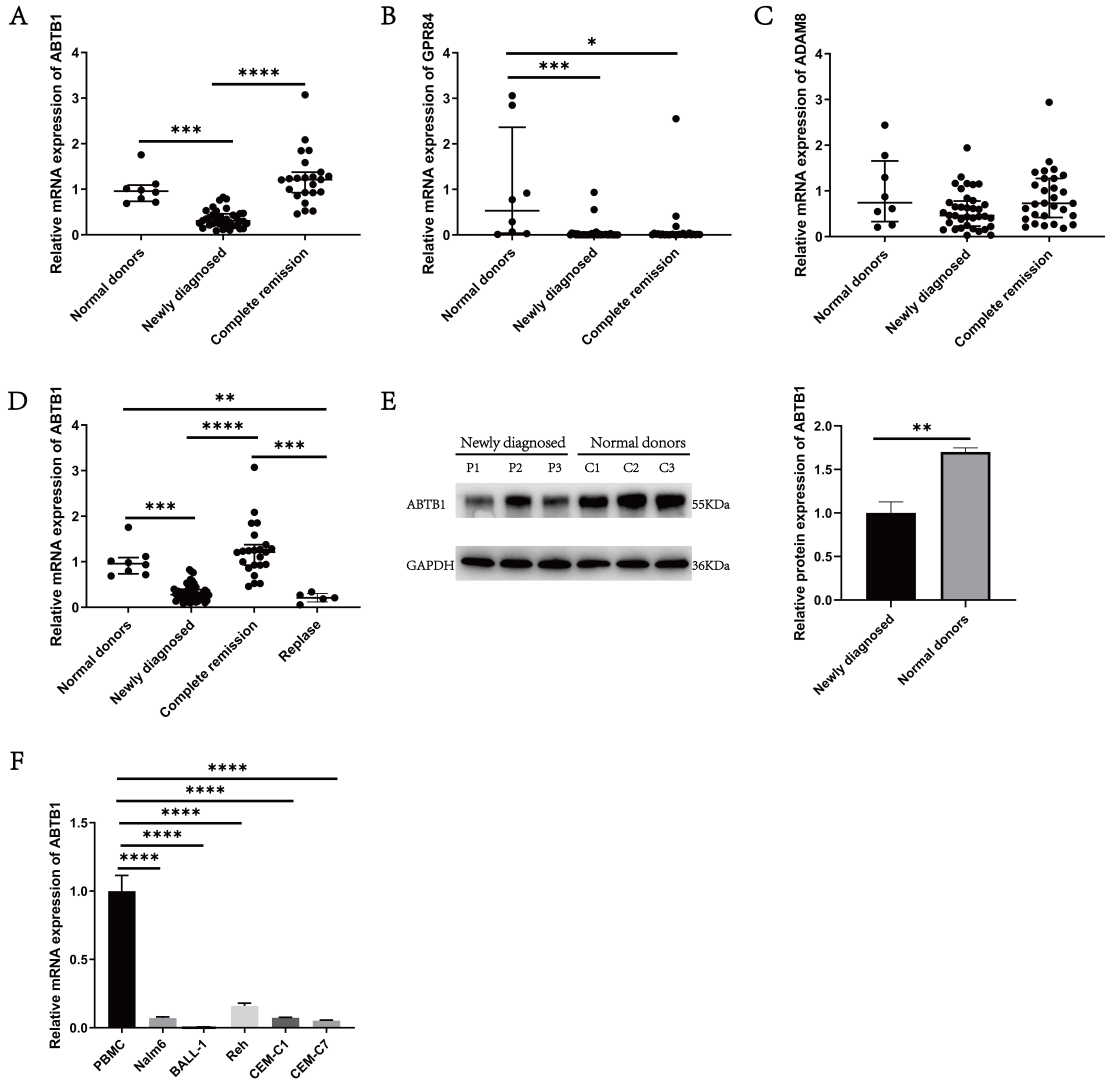

Fig. 5. Expression of ABTB1 in B-ALL specimens and cell lines. (A) mRNA levels of *ABTB1* were determined by RT-qPCR in newly diagnosed B-ALL patient samples (n = 36), the complete remission group (n = 23), and control subjects (n = 8). (B) mRNA levels of *GPR84* were determined by RT-qPCR in newly diagnosed B-ALL patient samples (n = 36), the complete remission group (n = 27), and control subjects (n = 8). (C) mRNA levels of *ADAM8* were determined by RT-qPCR in newly diagnosed B-ALL patient samples (n = 36), the complete remission group (n = 29), and control subjects (n = 8). (D) mRNA levels of ABTB1 were determined by RT-qPCR in newly diagnosed B-ALL patients (n = 36), the relapsed B-ALL patients (n = 5), the complete remission group (n = 23), and control subjects (n = 8). (E) Comparison of ABTB1 protein expression levels between the newly diagnosed B-ALL patients (n = 3) and control subjects (n = 3). (F) mRNA levels of *ABTB1* were determined by RT-qPCR in ALL cell lines relative to peripheral blood mononuclear cells (PBMC), conducted in triplicates. ****$p < 0.0001$, ***$p < 0.001$, **$p < 0.01$, *$p < 0.05$. GAPDH, Glyceraldehyde-3-phosphate dehydrogenase.

bioinformatics approaches, revealing a potential association between ABTB1 and recurrence in uveal melanoma patients. Collectively, these findings underscore the pivotal role of ABTB1 across various malignancies.

Despite the scarcity of reports on ABTB1 in acute leukemia mechanisms, as far back as 2000, Dai *et al.* [38] had postulated that ABTB1 exerts a significant influence on leukemia development due to its location on chromosomal locus 3q21, an area commonly associated with leukemia. In this study, we observed downregulation of ABTB1 in newly diagnosed and relapsed B-ALL patients compared to the control or complete remission group. Additionally, we identified correlations between the downregulation and clinical characteristics. These findings suggest that ABTB1 is predominantly expressed in normal cells rather than immature lymphocytes in pediatric B-ALL patients. Moreover, it is hypothesized that ABTB1 plays a significant role in inhibiting cell growth and proliferation.

Table 5. Relationship between clinical characteristics and ABTB1 mRNA levels in B-ALL patients.

Parameters	Number	ABTB1 Expression		*p*-value (χ^2)
		High	Low	
Age (years)				$p = 1.000$ (0.000)
≤10	38	19	19	
>10	2	1	1	
Gender				$p = 0.752$ (0.100)
Male	21	10	11	
Female	19	10	9	
WBC ($\times 10^9$/L)				$p = 0.047$ (3.956)
≤30	26	16	10	
>30	14	4	10	
PLT ($\times 10^9$/L)				$p = 0.168$ (1.905)
<100	28	12	16	
≥100	12	8	4	
BLAST in Bone Marrow (%)				$p = 0.548$ (0.360)
≤50	3	2	1	
>50	37	18	19	
Anemia				$p = 0.311$ (1.026)
Yes	39	20	19	
No	1	0	1	
Risk Classification				$p = 0.018$ (5.584)
Low and Middle	27	17	10	
High	13	3	10	
Gene Mutation				$p = 0.702$
Abnormal	12	6	6	
Normal	16	10	6	
Fusion Gene				$p = 1$
Abnormal	12	6	6	
Normal	25	12	13	
Karyotype				$p = 0.453$
Abnormal	12	4	8	
Normal	14	7	7	

Note: The association between *ABTB1* mRNA levels and karyotype, fusion gene, gene mutation was assessed by a Fisher's exact test.

Table 6. Correlations between clinical characteristics and ABTB1 mRNA levels in B-ALL patients.

Variables	ABTB1 expression level	*p*-value
	Spearman correlation	
Age (years)	0.078	0.632
Gender	0.102	0.531
WBC ($\times 10^9$/L)	–0.386	0.014
HGB (g/L)	0.016	0.921
PLT ($\times 10^9$/L)	0.247	0.125
BLAST in Bone Marrow (%)	–0.311	0.051
Anemia	–0.088	0.593
Risk Classification	–0.429	0.006
Mutation	–0.107	0.587
Fusion	–0.111	0.512
Karyotype	–0.051	0.803

HGB, hemoglobin.

Additionally, Kaplan-Meier survival curves demonstrated that low ABTB1 expression correlates with poor prognosis in B-ALL patients within the TARGET database. These findings indicate that the downregulation of ABTB1 may be responsible for the onset and progression of B-ALL as a tumor suppressor gene and represents a potentially novel prognostic marker for OS and a prospective therapeutic target for B-ALL treatment. However, there are some limitations in our study. First, our study is limited by a small sample size, which may impact statistical robustness. Second, we did not analyze the regulation pattern of ABTB1 using other RNA-seq data, as the Gene Expression Omnibus (GEO) database related to childhood B-ALL lacks data from healthy donors. Thus, further validation is warranted in a prospective nationwide project with a larger sample size. Additionally, we intend to explore the unknown mechanisms underlying the role of ABTB1 in B-ALL in future research endeavors, using cell and animal experiments for a more comprehensive understanding. This research offers a basis for developing targeted drug therapies for B-ALL.

Journal of
BIOLOGICAL REGULATORS
and Homeostatic Agents

Conclusions

In conclusion, our research identifies ABTB1 as a novel and significant contributor to B-ALL, with its down-regulation potentially promoting disease progression. Our findings indicate that ABTB1 holds promise as a novel prognostic biomarker in B-ALL.

Availability of Data and Materials

The data used to support the findings of our study are free access to available from the corresponding authors.

Author Contributions

Design: YL, YC and ZH; Data acquisition: YL; Methodology: YL, CL, PH, JW, XX; Data analysis and interpretation: YL; Writing (original draft): YL; Writing (review and editing): YL, YC, ZH. All authors contributed to editorial changes in the manuscript. All authors read and approved the final manuscript. All authors have participated sufficiently in the work and agreed to be accountable for all aspects of the work.

Ethics Approval and Consent to Participate

The ethic approval was obtained from the Ethic Committee of the Affiliated Hospital of Zunyi Medical University (KLL-2021-353). In compliance with the guidelines of the Declaration of Helsinki, informed consent was obtained from all participants.

Acknowledgment

We are grateful to the contributors of data to the TARGET database. We also would like to thank the many clinical doctors and experimenter from the Affiliated Hospital of Zunyi Medical University, who were involved in this study.

Funding

This study was supported by the National Natural Science Foundation of China (32270848), collaborative Innovation Center of Chinese Ministry of Education (2020-39), Guizhou Provincial Science and Technology Projects (QKHPTRC-CXTD[2021]010). Zunyi Science and Technology Plan Project (ZSKHZ-2023-203, ZSKRPT-2023-6, ZSKHZ-2021-186).

Conflict of Interest

The authors declare no conflict of interest.

Supplementary Material

Supplementary material associated with this article can be found, in the online version, at https://doi.org/10.23812/j.biol.regul.homeost.agents.20243806.369.

References

[1] Chiarini F, Paganelli F, Martelli AM, Evangelisti C. The Role Played by Wnt/β-Catenin Signaling Pathway in Acute Lymphoblastic Leukemia. International Journal of Molecular Sciences. 2020; 21: 1098.

[2] Malard F, Mohty M. Acute lymphoblastic leukaemia. Lancet. 2020; 395: 1146–1162.

[3] Chang JHC, Poppe MM, Hua CH, Marcus KJ, Esiashvili N. Acute lymphoblastic leukemia. Pediatric Blood & Cancer. 2021; 68: e28371.

[4] Siegel R, Naishadham D, Jemal A. Cancer statistics, 2012. CA: A Cancer Journal for Clinicians. 2012; 62: 10–29.

[5] Wei MC, Cleary ML. Novel methods and approaches to acute lymphoblastic leukemia drug discovery. Expert Opinion on Drug Discovery. 2014; 9: 1435–1446.

[6] Hunger SP, Mullighan CG. Acute Lymphoblastic Leukemia in Children. The New England Journal of Medicine. 2015; 373: 1541–1552.

[7] Inaba H, Pui CH. Advances in the Diagnosis and Treatment of Pediatric Acute Lymphoblastic Leukemia. Journal of Clinical Medicine. 2021; 10: 1926.

[8] Inaba H, Mullighan CG. Pediatric acute lymphoblastic leukemia. Haematologica. 2020; 105: 2524–2539.

[9] Bhojwani D, Howard SC, Pui CH. High-risk childhood acute lymphoblastic leukemia. Clinical Lymphoma & Myeloma. 2009; 9: S222–S230.

[10] Jeha S, Pei D, Choi J, Cheng C, Sandlund JT, Coustan-Smith E, *et al*. Improved CNS Control of Childhood Acute Lymphoblastic Leukemia Without Cranial Irradiation: St Jude Total Therapy Study 16. Journal of Clinical Oncology. 2019; 37: 3377–3391.

[11] Mengxuan S, Fen Z, Runming J. Novel Treatments for Pediatric Relapsed or Refractory Acute B-Cell Lineage Lymphoblastic Leukemia: Precision Medicine Era. Frontiers in Pediatrics. 2022; 10: 923419.

[12] Iacobucci I, Mullighan CG. Genetic Basis of Acute Lymphoblastic Leukemia. Journal of Clinical Oncology. 2017; 35: 975–983.

[13] Shen S, Chen X, Cai J, Yu J, Gao J, Hu S, *et al*. Effect of Dasatinib vs Imatinib in the Treatment of Pediatric Philadelphia Chromosome-Positive Acute Lymphoblastic Leukemia: A Randomized Clinical Trial. JAMA Oncology. 2020; 6: 358–366.

[14] Slayton WB, Schultz KR, Kairalla JA, Devidas M, Mi X, Pulsipher MA, *et al*. Dasatinib Plus Intensive Chemotherapy in Children, Adolescents, and Young Adults with Philadelphia Chromosome-Positive Acute Lymphoblastic Leukemia: Results of Children's Oncology Group Trial AALL0622. Journal of Clinical Oncology. 2018; 36: 2306–2314.

[15] Tse C, Shoemaker AR, Adickes J, Anderson MG, Chen J, Jin S, *et al*. ABT-263: a potent and orally bioavailable Bcl-2 family inhibitor. Cancer Research. 2008; 68: 3421–3428.

[16] Pullarkat VA, Lacayo NJ, Jabbour E, Rubnitz JE, Bajel A, Laetsch TW, *et al*. Venetoclax and Navitoclax in Combination with Chemotherapy in Patients with Relapsed or Refractory Acute Lymphoblastic Leukemia and Lymphoblastic Lymphoma. Cancer Discovery. 2021; 11: 1440–1453.

[17] McEwan A, Pitiyarachchi O, Viiala N. Relapsed/Refractory ETP-ALL Successfully Treated with Venetoclax and Nelarabine as a Bridge to Allogeneic Stem Cell Transplant. HemaSphere. 2020; 4: e379.

[18] Jovic D, Liang X, Zeng H, Lin L, Xu F, Luo Y. Single-cell RNA sequencing technologies and applications: A brief overview. Clinical and Translational Medicine. 2022; 12: e694.

[19] Rahmani M, Talebi M, Hagh MF, Feizi AAH, Solali S. Aberrant DNA methylation of key genes and Acute Lymphoblastic Leukemia. Biomedicine & Pharmacotherapy. 2018; 97: 1493–1500.

[20] Gu Z, Churchman ML, Roberts KG, Moore I, Zhou X, Nakitandwe J, *et al*. PAX5-driven subtypes of B-progenitor acute lymphoblastic leukemia. Nature Genetics. 2019; 51: 296–307.
[21] Mullighan CG, Su X, Zhang J, Radtke I, Phillips LAA, Miller CB, *et al*. Deletion of IKZF1 and prognosis in acute lymphoblastic leukemia. The New England Journal of Medicine. 2009; 360: 470–480.
[22] Lejman M, Chałupnik A, Chilimoniuk Z, Dobosz M. Genetic Biomarkers and Their Clinical Implications in B-Cell Acute Lymphoblastic Leukemia in Children. International Journal of Molecular Sciences. 2022; 23: 2755.
[23] Xu J, Zhao L. Polo-like Kinase 4: the Variation During Therapy and its Relation to Treatment Response and Prognostic Risk Stratification in Childhood Acute Lymphoblastic Leukemia Patients. Journal of Pediatric Hematology/Oncology. 2023; 45: 189–194.
[24] Smaldone G, Beneduce G, Incoronato M, Pane K, Franzese M, Coppola L, *et al*. KCTD15 is overexpressed in human childhood B-cell acute lymphoid leukemia. Scientific Reports. 2019; 9: 20108.
[25] Luo Y, Xu Y, Li X, Shi X, Huang P, Chen Y, *et al*. A Prognostic Model of Seven Immune Genes to Predict Overall Survival in Childhood Acute Myeloid Leukemia. BioMed Research International. 2022; 2022: 7724220.
[26] Doncheva NT, Morris JH, Gorodkin J, Jensen LJ. Cytoscape StringApp: Network Analysis and Visualization of Proteomics Data. Journal of Proteome Research. 2019; 18: 623–632.
[27] Shannon P, Markiel A, Ozier O, Baliga NS, Wang JT, Ramage D, *et al*. Cytoscape: a software environment for integrated models of biomolecular interaction networks. Genome Research. 2003; 13: 2498–2504.
[28] Chin CH, Chen SH, Wu HH, Ho CW, Ko MT, Lin CY. cytoHubba: identifying hub objects and sub-networks from complex interactome. BMC Systems Biology. 2014; 8: S11.
[29] Medinger M, Heim D, Lengerke C, Halter JP, Passweg JR. Acute lymphoblastic leukemia - diagnosis and therapy. Therapeutische Umschau. Revue Therapeutique. 2019; 76: 510–515. (In German)
[30] Henze G, v Stackelberg A, Eckert C. ALL-REZ BFM–the consecutive trials for children with relapsed acute lymphoblastic leukemia. Klinische Padiatrie. 2013; 225: S73–S78.
[31] Moorman AV. New and emerging prognostic and predictive genetic biomarkers in B-cell precursor acute lymphoblastic leukemia. Haematologica. 2016; 101: 407–416.
[32] Wyatt KD, Bram RJ. Immunotherapy in pediatric B-cell acute lymphoblastic leukemia. Human Immunology. 2019; 80: 400–408.
[33] Jasinski S, De Los Reyes FA, Yametti GC, Pierro J, Raetz E, Carroll WL. Immunotherapy in Pediatric B-Cell Acute Lymphoblastic Leukemia: Advances and Ongoing Challenges. Paediatric Drugs. 2020; 22: 485–499.
[34] Pierro J, Hogan LE, Bhatla T, Carroll WL. New targeted therapies for relapsed pediatric acute lymphoblastic leukemia. Expert Review of Anticancer Therapy. 2017; 17: 725–736.
[35] Santiago R, Vairy S, Sinnett D, Krajinovic M, Bittencourt H. Novel therapy for childhood acute lymphoblastic leukemia. Expert Opinion on Pharmacotherapy. 2017; 18: 1081–1099.
[36] Place AE, Pikman Y, Stevenson KE, Harris MH, Pauly M, Sulis ML, *et al*. Phase I trial of the mTOR inhibitor everolimus in combination with multi-agent chemotherapy in relapsed childhood acute lymphoblastic leukemia. Pediatric Blood & Cancer. 2018; 65: e27062.
[37] Brown P, Pieters R, Biondi A. How I treat infant leukemia. Blood. 2019; 133: 205–214.
[38] Dai KS, Wei W, Liew CC. Molecular cloning and characterization of a novel human gene containing ankyrin repeat and double BTB/POZ domain. Biochemical and Biophysical Research Communications. 2000; 273: 991–996.
[39] Unoki M, Nakamura Y. Growth-suppressive effects of BPOZ and EGR2, two genes involved in the PTEN signaling pathway. Oncogene. 2001; 20: 4457–4465.
[40] Huang L, Zhang Y, Li Z, Zhao X, Xi Z, Chen H, *et al*. MiR-4319 suppresses colorectal cancer progression by targeting ABTB1. United European Gastroenterology Journal. 2019; 7: 517–528.
[41] Wan Q, Tang J, Han Y, Wang D. Co-expression modules construction by WGCNA and identify potential prognostic markers of uveal melanoma. Experimental Eye Research. 2018; 166: 13–20.